

FDM SIMULATION OF LASER-INDUCED CRATER FORMATION

INTRODUCTION

Lasers are being used in more and more industries; the field of laser-material interactions has advanced significantly. The ablation of metals with nanosecond laser sources has become popular among the many processes that lasers provide. By absorbing pulsed laser light, material can be removed from a surface in a using laser ablation and is much cheaper as compared to fs or ps lasers. This process plays a important role in numerous applications, ranging from material processing to and scientific research. [3] The laser-material interaction studied in this report involves the application of a nanosecond (ns) laser source onto a thin SS316 plate. The primary processing mechanism in this interaction is thermal. The incident laser pulse is absorbed near the workpiece's surface, creating a volume heat source. This study takes the advantage of the explicit Finite Difference Method (FDM) to develop a two-dimensional numerical model, aiming to understand the thermal dynamics, material removal rate, and associated side effects (HAZ) during laser ablation. Laser ablation is a popular research topic, and a lot of research is being done on this topic currently. Few of the topics are cited in bibliography.

Aims and Objectives

Aim of the report is to develop a numerical model to simulate the interactions between a nanosecond laser source and metallic materials. And to simulate laser ablation of a single nano second laser pulse, in Matlab, resulting in formation of a crated that can be validated with provided experimental results. Find the HAZ of the interaction and approximating the temperature distribution across the workpiece.

METHODOLOGY

The model is based on conventional heat diffusion equation with heat source i.e. a single ns laser pulse with Gaussian temporal and spatial profiles. The relationship between temperature, energy density, and the state change of the material is considered in the model. Latent heat of evaporation is ignored because it is assumed that liquid to gas transition removes material, however latent heat of diffusion is considered.

The governing physics

The governing physics in the context of laser-material interaction involve the fundamental principles of heat transfer and phase change. The equations governing these physics are derived from principles in heat conduction, absorption of electromagnetic radiation, and phase change dynamics.

Heat Conduction

Using Heat Conduction Equation - a partial differential equation that describes heat distribution (or the temperature field) in a given body over time.

$$\rho C_p \frac{\partial T}{\partial t} = K \nabla(\Delta T) + Q \quad [1]$$

where ρ is the material density, C_p is the heat capacity, K is the thermal conductivity, T is the temperature, t is time, and ∇ is the del operator.

The general heat conduction equation in two dimensions:

$$\rho C_p \frac{\partial T(x, z, t)}{\partial t} = K \left(\frac{\partial^2 T}{\partial x^2} + \frac{\partial^2 T}{\partial z^2} \right) + A(x, z, t) [1]$$

Absorption of Pulse Energy (electromagnetic radiation):

The absorption process is described by the Beer-Lambert law, considering the material's absorption characteristics. Here, $A(x, z, t)$ is the volume heat source (the absorbed laser energy in a given unit of a material volume).

$$A(x, z, t) = \alpha I_0 p(t, x) e^{-\alpha z}$$

Here $p(t, x)$ is spatial and temporal profile. The governing equation for the absorbed pulse energy accounting for the absorption coefficient α , laser intensity I_0 , and temporal and spatial profiles of the laser pulse $p(t, x)$ is given as:

$$\rho C_p \frac{\partial T(x, z, t)}{\partial t} = K \left(\frac{\partial^2 T}{\partial x^2} + \frac{\partial^2 T}{\partial z^2} \right) + \alpha I_0 p(t, x) e^{-\alpha z}$$

Rearranging,

$$\frac{\partial T(x, z, t)}{\partial t} = \frac{K}{\rho C_p} \left(\frac{\partial^2 T}{\partial x^2} + \frac{\partial^2 T}{\partial z^2} \right) + \frac{1}{\rho C_p} \alpha I_0 p(t, x) e^{-\alpha z}$$

Finite Difference Method (FDM)

Now, discretize the governing equations using the explicit forward Finite Difference Method of derivatives, derived from the Taylor series, for numerical simulation. Let $T_{i,k}$ represents the temperature at grid point (i, k) .

The temporal and spatial derivatives can be approximated as follows: [1]

$$\begin{aligned} \frac{\partial T(x, z, t)}{\partial t} &\approx \frac{T_{i,k}^{n+1} - T_{i,k}^n}{\Delta t} \\ \frac{\partial^2 T}{\partial x^2} &\approx \frac{T_{i+1,k}^n - 2T_{i,k}^n + T_{i-1,k}^n}{\Delta x^2} \\ \frac{\partial^2 T}{\partial z^2} &\approx \frac{T_{i,k+1}^n - 2T_{i,k}^n + T_{i,k-1}^n}{\Delta z^2} \end{aligned}$$

Substituting the values of $\frac{\partial^2 T}{\partial x^2}$, $\frac{\partial^2 T}{\partial z^2}$ and $\frac{\partial T(x,z,t)}{\partial t}$ into the partial differential equation.

$$\frac{T_{i,k}^{n+1} - T_{i,k}^n}{\Delta t} = \frac{K}{\rho C_p} \left(\frac{T_{i+1,k}^n - 2T_{i,k}^n + T_{i-1,k}^n}{\Delta x^2} + \frac{T_{i,k+1}^n - 2T_{i,k}^n + T_{i,k-1}^n}{\Delta z^2} \right) + \frac{1}{\rho C_p} \alpha I_0 p(t, x) e^{-\alpha z}$$

Rearranging the explicit FDM equation for heat conduction is used to update the temperature field at each time step.

$$T_{i,k}^{n+1} = T_{i,k}^n + \frac{\Delta t K}{\rho C_p} \left(\frac{T_{i+1,k}^n - 2T_{i,k}^n + T_{i-1,k}^n}{\Delta x^2} + \frac{T_{i,k+1}^n - 2T_{i,k}^n + T_{i,k-1}^n}{\Delta z^2} \right) + \frac{\Delta t}{\rho C_p} \alpha I_0 p(t, x) e^{-\alpha z}$$

Temporal and Spatial profiles of Beam

A beam with Gaussian temporal and spatial profiles is used for this laser-material interaction experiment. For beams with Gaussian temporal and spatial profiles $p(t, x)$ is:

$$p(t, x) = \int e^{-\left(\frac{x}{R_0}\right)^2} \int e^{-\left(\frac{t}{\tau}\right)^2}$$

Here R_0 is beam radius at focus, τ is pulse duration, t is time.

Iterative equation:

$$T_{i,k}^{n+1} = T_{i,k}^n + \frac{\Delta t K}{\rho C p} \left(\frac{T_{i+1,k}^n - 2T_{i,k}^n + T_{i-1,k}^n}{\Delta x^2} + \frac{T_{i,k+1}^n - 2T_{i,k}^n + T_{i,k-1}^n}{\Delta z^2} \right) + \frac{\Delta t}{\rho C p} \alpha I_0 e^{-\left(\frac{x}{R_0}\right)^2} e^{-\left(\frac{t}{\tau}\right)^2} e^{-\alpha z}$$

The equation is explicit as the known temperature at the previous step in time determine unknown temperatures for the next time step $i + 1$. The next step in time is calculated by $\Delta t = \tau/10$ or the following formula whichever is smallest.

$$\Delta t \leq 0.5 \times \frac{\rho C_p \Delta x^2 \Delta z^2}{K(\Delta x^2 + \Delta z^2)}$$

First row equation

The equation for estimating temperature in first row is obtained by substituting the term $T_{i-1,k}^n$ with ambient temperature.

$$T_{i,k}^{n+1} = T_{i,k}^n + \frac{\Delta t K}{\rho C p} \left(\frac{T_{i+1,k}^n - 2T_{i,k}^n + T_0^n}{\Delta x^2} + \frac{T_{i,k+1}^n - 2T_{i,k}^n + T_{i,k-1}^n}{\Delta z^2} \right) + \frac{\Delta t}{\rho C p} \alpha I_0 e^{-\left(\frac{x}{R_0}\right)^2} e^{-\left(\frac{t}{\tau}\right)^2} e^{-\alpha z}$$

Assumptions:

- Steady-state conditions are assumed.
- A rectangular grid with indices i, k representing spatial coordinates x, z respectively.
- The material properties (density ρ , heat capacity C_p , thermal conductivity K) are assumed to be constant.
- Ambient temperature is 20°C.

Phase Change:

The model also incorporates adjustments for latent heat of fusion during phase changes from solid to liquid. However, latent heat of evaporation is ignored because it is assumed that liquid to gas transition removes material. In simulation a mask is applied to store points where adjustment has already made to avoid making adjustment every time the loop runs.

$$T_{new} = T_{old} - \frac{L_m}{C_p} [2]$$

Simulation

The code starts with defining parameters such as material properties, laser parameters and simulation details. The metallic segment of $400\mu\text{m}$ in length and $80\mu\text{m}$ in depth is discretized in both spatial X, Z dimensions using the FDM. A grid to represent the plate is created as a Matrix.

The absorbed pulse energy is calculated at each grid point using the absorption coefficient, laser intensity, and the temporal-spatial profile of the laser pulse. This accounts for how much energy is being deposited into the material. The heat conduction equation is discretized and solved at each time step.

At each time step, the code checks if the temperature at any point has reached the melting point. If so, it adjusts the temperature to account for the latent heat of melting. A mask is applied to store points where adjustment has already made to avoid making adjustment every time the loop runs.

The simulation begins at the start of pulse and maximum laser intensity occurs at $t = 0.5 \tau$ (pulse duration), aligning with the pulse duration τ for simplicity. The simulation iterates through multiple time steps, updating the temperature distribution based on the absorbed pulse energy, heat conduction, and any adjustments for phase change.

RESULTS

The detailed contour plots showing the evolving temperature distribution and crater depth in the Z direction is obtained as a result of simulation. These plots are generated at regular intervals, specifically every step Δt in the pulse duration. The visualization provides a comprehensive understanding of how the material responds to the single laser pulse over time (0ns - 140ns).

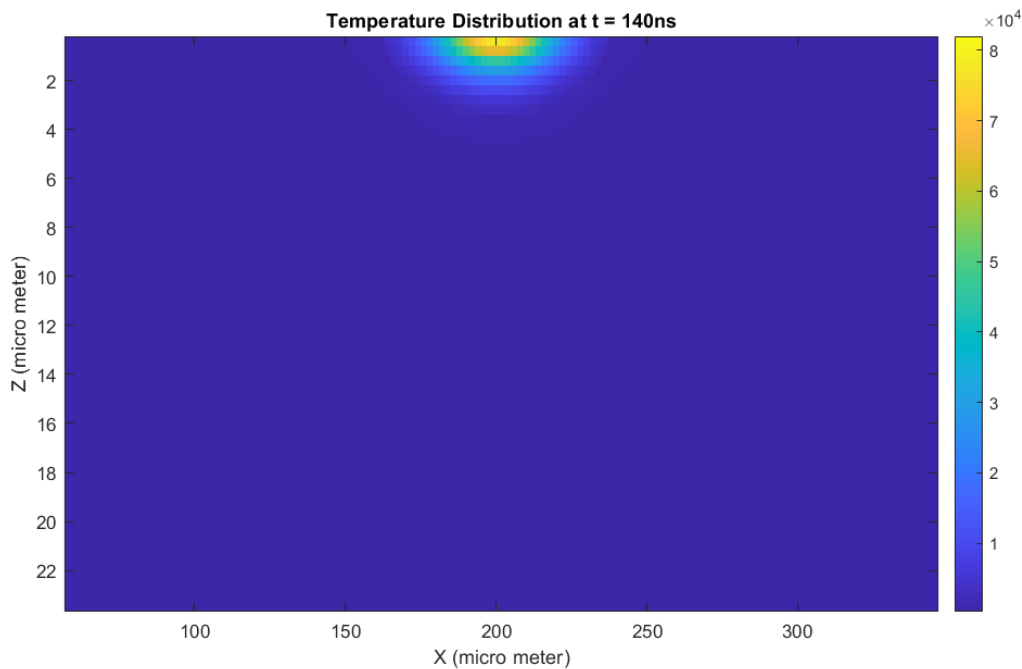


Figure 1: Temperature Distribution at time 140ns

Material Properties

The table below summarizes the physical, optical, and thermal properties of SS 316.

Table 1: Material Properties

<i>Properties</i>	<i>Symbol</i>	<i>Value</i>	<i>Unit</i>
Melting Point	T _m	1670	K
Boiling Point	T _b	3173	K
Density	Rho	8238	Kg/m ³
Specific-heat capacity	μ _m	468	J/kg K
Thermal conductivity	K	13.4	W/m K
Latent heat of melting	L _f	3.0+5	J/K
Absorption coefficient	alpha	5.45e+7	1/m

Model Validation

To validate the model against the available experimental results. The data is exported in excel to find the exact point in material where the temperature has raised above the boiling point.

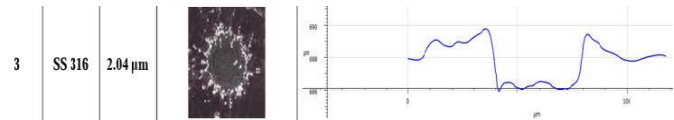


Figure 2: Provided Experimental data

Index	82	83	84	85	86	87	88	89	90	91	92	93	94	95	96	97	98	99	100	101	102	103	104	105	106	107	108	109	110	111	112	113	114	115	116	117	118	119
1	1831	3228	4526	6219	8403	11180	14591	18674	23451	28886	34888	41318	47966	54593	60915	66630	71446	75096	77378	75112	71469	66660	60948	54629	48003	41354	34923	28918	23480	18688	14612	11198	8417	6230	4537	3235	1823	634
2	680	2387	3757	5123	6976	9301	12159	15579	19591	24142	29174	34568	40138	45896	50997	55790	59827	62887	64834	62919	59872	55846	51061	45766	40209	34638	29241	24203	19646	15628	12200	9334	7003	5144	3777	2391	684	1254
3	1136	865	2644	3513	4844	6409	8417	10813	13608	16772	20288	24056	27945	31825	35526	38874	41688	43829	45170	43868	41744	38943	35606	31910	28033	24143	20371	16848	13675	10872	8468	6450	4877	3540	2467	877	1153	1016
4	905	1193	1144	2295	2968	4083	5412	6920	8730	10786	13082	15509	18038	20548	22949	25121	26944	28341	29214	28379	26999	25190	23028	20633	18125	15594	13163	10862	8798	6977	5460	4127	3001	2312	872	1205	917	787
5	698	888	1200	1495	1722	2523	3150	4132	5295	6586	7957	9439	11005	12560	14038	15377	16511	17380	17919	17413	16558	15436	14106	12633	11079	9513	8026	6649	5353	4185	3192	2553	1753	1519	1130	900	708	609
6	544	659	826	1002	1204	1569	1749	2417	3127	3700	4561	5477	6405	7350	8163	8853	9639	10156	10474	10182	9675	8998	8214	7404	6462	5534	4618	3748	3168	2454	1784	1600	1226	1019	812	668	551	485
7	441	506	596	699	829	1014	1182	1486	1215	1990	2568	3114	3445	3986	4496	4946	5343	5638	5819	5657	5369	4978	4537	4028	3483	3151	2605	2028	1250	1514	1206	1034	845	710	596	513	446	405
8	376	412	460	518	593	690	799	952	1144	1280	1523	1152	1783	2072	2449	2695	2911	3072	3173	3085	2929	2716	2473	2098	1814	1183	1549	1304	1165	971	814	703	603	526	463	416	380	356
9	338	357	383	414	455	506	568	648	746	835	950	1084	1144	1288	1424	1554	1666	1109	1151	1117	1036	1567	1440	1306	1161	1102	966	850	759	659	578	514	461	419	385	360	340	327
10	317	327	340	357	378	405	438	479	529	579	636	703	751	823	882	949	1005	1047	1074	1052	1011	958	892	833	761	713	646	588	536	486	443	409	382	359	342	328	318	311
11	305	310	317	326	337	350	367	388	413	440	468	501	531	566	595	629	655	676	690	679	659	633	600	571	536	507	474	445	417	392	370	353	339	327	318	311	306	302
12	299	302	305	309	315	322	330	341	353	367	381	397	413	429	444	461	474	484	490	485	476	464	447	433	416	400	384	369	355	343	332	323	316	310	306	302	300	298
13	296	297	299	301	304	307	311	316	322	329	336	344	352	360	367	376	382	386	389	387	383	377	369	362	354	346	338	331	324	318	312	308	304	302	299	298	296	295
14	295	295	296	297	298	300	302	304	307	310	314	317	321	325	329	333	336	338	339	338	336	334	330	326	322	318	315	311	308	305	302	300	299	297	296	295	295	294

Figure 3:Temperature data of the area of interest of workpiece

$$\text{Crater Depth} = \text{Number of rows above the boiling point} \times \Delta z$$

$$\text{Crater Depth} = 6 \times 0.4\mu\text{m} = \mathbf{2.4\mu\text{m}}$$

The crater depth provided in the experimental data is 2.04 μm. Whereas results obtained from simulation is 2.4 μm. The difference among them is 15%. The depth obtained from simulation is 15% more than the experiment. Which is close enough to be used for our results.

Crater Depth at Δt steps in time.

Table 2: Crater Depth at different time steps

t	Number of rows above T_b	Crater depth	Crater depth
0ns	0	$0 \times 0.4\mu\text{m}$	$0\mu\text{m}$
14ns	1	$1 \times 0.4\mu\text{m}$	$0.4\mu\text{m}$
28ns	2	$2 \times 0.4\mu\text{m}$	$0.8\mu\text{m}$
42ns	3	$3 \times 0.4\mu\text{m}$	$1.2\mu\text{m}$
56ns	3	$3 \times 0.4\mu\text{m}$	$1.2\mu\text{m}$
70ns	4	$4 \times 0.4\mu\text{m}$	$1.6\mu\text{m}$
84ns	4	$4 \times 0.4\mu\text{m}$	$1.6\mu\text{m}$
98ns	4	$4 \times 0.4\mu\text{m}$	$1.6\mu\text{m}$
112ns	5	$5 \times 0.4\mu\text{m}$	$2.0\mu\text{m}$
126ns	5	$5 \times 0.4\mu\text{m}$	$2.0\mu\text{m}$
140ns	6	$6 \times 0.4\mu\text{m}$	$2.4\mu\text{m}$

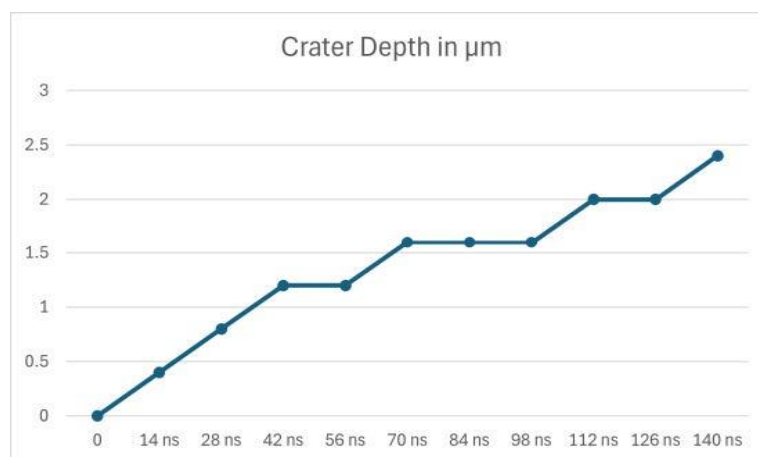


Figure 4: Crater depth in μm

$$\text{Crater Diameter} = \text{Number of columns above the boiling point} \times \Delta x$$

$$\text{Crater Depth} = 35 \times 2\mu\text{m} = \mathbf{70\mu\text{m}}$$

Material Removal Rate (MRR)

To calculate the material removal rate following formula can be used. Since volume is not modelled in simulation and it deals with area only. Material removal rate can't be estimated exactly.

$$\text{Material Removal Rate (MRR)} = \text{Volume Removed} / \text{Pulse Duration}$$

DISCUSSION

The discussion interprets the simulation results, emphasizing the influence of laser material interaction parameters such as power, pulse duration, and material absorptivity on temperature distribution and crater depth. The spatial and temporal profiles of the laser pulse are analysed for their impact on the heat affected zone and crater depth in the material. The effects of latent heat during phase transitions are scrutinized, highlighting their importance in accurately predicting material behaviour that validates with the experimental results.

Crater Formation

To find the crater depth, the data of temperature distribution is subtracted from evaporation point of material resulting in formation of a mask which is then plotted to make the crater. In this picture formation of crater can be seen clearly.

Exact crater depth calculation is made on excel at Δt steps in time and graph of area of interest is plotted on xz plane.

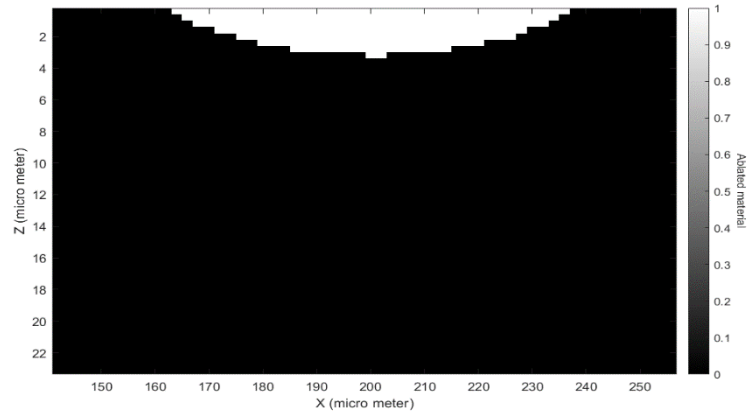


Figure 5: Formation of Crater

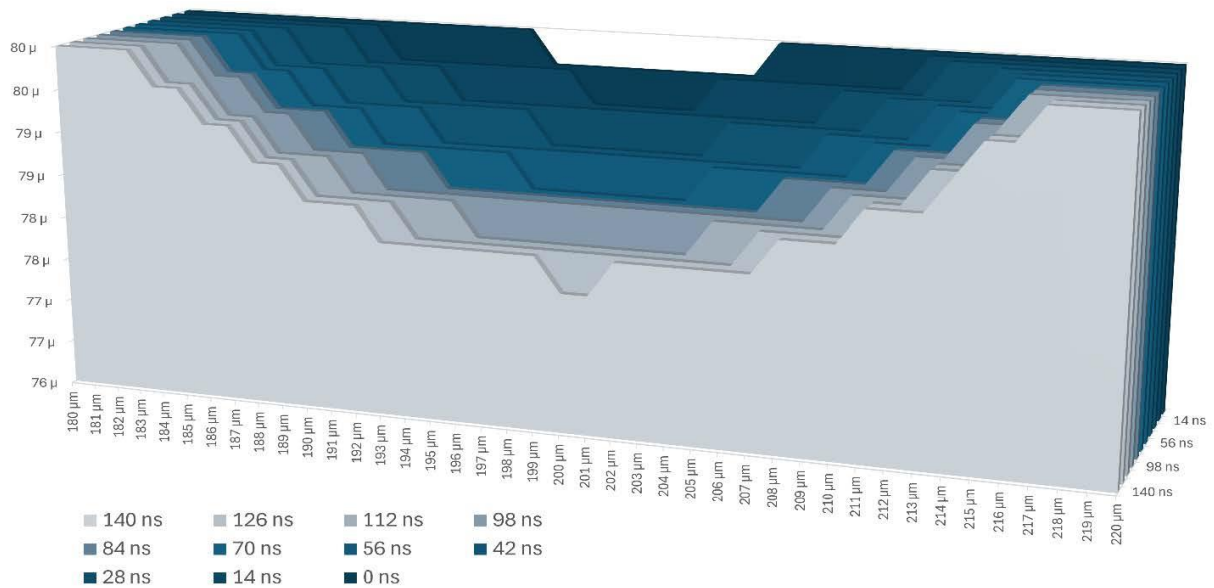


Figure 6: Simulation of crater depths obtained at Δt steps in time

Heat Affected Zone

The heat-affected zone (HAZ) in laser ablation is typically defined as the region in the material where the temperature rises significantly but doesn't reach the threshold for material removal or vaporization. It is the region that experiences thermal changes without undergoing significant physical changes. Localized thermal load and heat affected zone can be calculated given the temperature threshold. In simulation it can be modelled the similar way crater formation is modelled. If threshold is assumed $0.7T_m$ the Heat Affected Cells are given as yellow-coloured

cells in the picture of excel sheet below. Multiply the number of affected cells with dx and dz, one can calculate exact dimensions of HAZ.

index	81	82	83	84	85	86	87	88	89	90	91	92	93	94	95	96	97	98	99	100	101	102	103	104	105	106	107	108	109	110	111	112	113	114	115	116	117	118	119	120
1	1831	3228	4526	6219	8403	11180	14591	18674	23451	28886	34888	41318	47966	54593	60915	66630	71446	75996	79738	82617	77386	75112	71469	66660	60948	54629	48003	41354	34923	28918	23480	18698	14612	11198	8417	6230	4537	3235	1823	634
2	680	2387	3757	5123	6976	9301	12159	15679	19691	24142	29174	34588	40138	45696	50997	55790	59827	62887	64804	65461	64820	62919	59872	55846	51061	45766	40209	34638	29241	24203	19646	15628	12200	9334	7003	5144	3777	2391	684	1254
3	1136	865	2644	3513	4844	6409	8417	10813	13608	16772	20288	24056	27945	31825	35526	38874	41688	43829	45170	45333	45190	43868	41744	38943	35606	31910	28033	24143	20371	16848	13675	10872	8468	6450	4877	3540	2467	877	1153	1016
4	905	1193	1144	2235	2968	4083	5412	6920	8730	10786	13082	15509	18038	20548	22949	25121	26944	28341	29214	29517	29234	28379	26999	25190	23028	20633	18125	15594	13163	10862	8798	6977	5460	4127	3001	2312	872	1205	917	787
5	698	888	1200	1495	1722	2523	3150	4132	5295	6586	7957	9439	11005	12560	14039	15377	16511	17380	17919	18091	17936	17413	16558	15436	14106	12633	11079	9513	8026	6649	5353	4185	3192	2553	1753	1319	1130	900	708	609
6	544	659	826	1002	1204	1569	1749	2417	3127	3700	4561	5477	6405	7350	8163	8953	9639	10156	10474	10567	10488	10182	9675	8998	8214	7404	6462	5534	4618	3748	3168	2454	1784	1600	1226	1319	812	668	551	485
7	441	506	596	699	829	1014	1182	1488	1215	1990	2568	3114	3445	3986	4486	4946	5343	5638	5819	5917	5829	5657	5369	4978	4537	4028	3483	3151	2605	2028	1250	1514	1206	1034	845	710	596	513	446	405
8	376	412	460	518	593	690	799	952	1144	1280	1523	1152	1783	2072	2449	2695	2911	3072	3173	3254	3178	3085	2929	2716	2473	2098	1814	1183	1549	1304	1165	971	814	703	603	526	463	416	380	356
9	338	357	383	414	455	506	568	648	746	835	950	1094	1144	1288	1424	1554	1666	1109	1161	1188	1165	1117	1036	1567	1440	1306	1161	1102	966	850	759	659	578	514	461	419	385	360	340	327
10	317	327	340	357	378	405	438	479	529	579	636	703	751	823	882	949	1005	1047	1074	1079	1077	1052	1011	958	892	833	761	713	646	588	536	486	443	409	382	359	342	328	318	311
11	305	310	317	326	337	350	367	388	413	440	468	501	531	566	595	629	655	676	690	689	691	679	659	633	600	571	536	507	474	445	417	392	370	353	339	327	318	311	306	302
12	299	302	305	309	315	322	330	341	353	367	381	397	413	429	444	461	474	484	490	490	491	485	476	464	447	433	416	400	384	369	355	343	332	323	316	310	306	302	300	298
13	296	297	299	301	304	307	311	316	322	329	336	344	352	360	367	376	382	386	389	389	390	387	383	377	369	362	354	346	338	331	324	318	312	308	304	302	299	298	296	295
14	295	295	296	297	298	300	302	304	307	310	314	317	321	325	329	333	336	338	339	339	339	338	336	334	330	326	322	318	315	311	308	305	302	300	299	297	296	295	295	294

Figure 7: Heat Affected Zone marked as Yellow Cells

CONCLUSIONS

In conclusion, the Explicit Finite Difference Method (FDM) is used to simulate nanosecond laser ablation of metals, and the results have provided understandings of the thermal aspects of the process. The majority of the material is removed by ablation when the laser is at peak intensity. The intensity exhibits a bell-shaped curve of a Gaussian temporal profile, peaking at the middle of the pulse duration. This suggests that this central period is where the critical material removal and thermal effects are concentrated.

The temperature distribution of the metallic plate affects greatly by introducing Latent heat of fusion. Spatial and temporal profile also play an important role in deciding when the maximum material is removed during the pulse duration and position of pulse. Depth decay is directly proportional to the depth of the material. It also changes with material and depends on the absorption coefficient of material.

A comprehensive understanding of the heat distribution across a thin metallic plate, allowing for predictions of cratered depth and assessments of thermal effects such as heat affected zone and layer development. The crater depth of the simulated example is $2.4\mu m$ and crater diameter is $70\mu m$. Which is very close to the provided experimental results. The simulation closely estimates the heat distribution across the thin metallic plate.

REFERENCE

- [1] I. (2009, July 1). Fundamentals Of Heat And Mass Transfer, 5Th Ed. John Wiley & Sons.
- [2] Dobrev, T., Dimov, S. S., & Thomas, A. J. (2006, November 1). Laser milling: Modelling crater and surface formation. Proceedings of the Institution of Mechanical Engineers, Part C: Journal of Mechanical Engineering Science, 220(11), 1685–1696.
<https://doi.org/10.1243/09544062jmes221>
- [3] Dutta Majumdar, J., & Manna, I. (2011, November). Laser material processing. International Materials Reviews, 56(5–6), 341–388.
<https://doi.org/10.1179/1743280411y.0000000003>
- [4] M.H. Mahdieh, M. Nikbakht, Z. Eghlimi Moghadam, M. Sobhani. "Crater geometry characterization of Al targets irradiated by single pulse and pulse trains of Nd:YAG laser in ambient air and water", Applied Surface Science, 2010

APPENDIX

MATLAB Code of the simulation is attached below

```
% Parameters
clear all;
rho = 8.238e3;      % Material density [kg/m^3]
Cp = 4.68e2;        % Heat capacity [J/kg*K]
Kappa = 1.34e1;      % Thermal conductivity [W/m*K]
alpha = 5.45e6;      % Absorption coefficient [m^-1]
Pav = 30;           % Average Power [W]
f = 1.02e5;          % Laser pulse frequency [Hz]
tau = 1.4e-7;        % Laser pulse duration [s]
w0 = 4e-5;           % Laser beam spot Ø [m]
Tm = 1.670e3;        % Melting point [K]
Tb = 3.173e3;        % Boiling point [K]
Lf = 3.0e5;          % Latent heat of melting (kJ/kg)
melting_mask = false(200,200); % Mask to apply temperature adjustment
melting_mask1 = false(200,200); % Mask to store last applied adjustment

R0 = w0 / 2;        % Radius of the laser beam spot at the focus [m]
I0 = Pav / (f * tau * pi * R0^2); % Peak on-line laser intensity [W/m^2]

% Spatial and temporal discretization
dx = 2e-6;          % Discretization along x axis [m]
dz = 4e-7;          % Discretization along z axis [m]
dt1 = 0.5*(rho*Cp*dx^2*dz^2)/(Kappa*(dx^2+dz^2)); % Time step (s)
dt2 = tau/10;
dt = min([dt1 dt2]);

Lx = 4e-4;          % Length of the material in x [m]
Lz = 8e-5;          % Length of the material in z [m]

Nx = round(Lx / dx); % Number of spatial grid points in X
Nz = round(Lz / dz); % Number of spatial grid points in Z
Nt = round(tau / dt); % Number of time steps

% Boundry Conditions
T0 = 293.15;        % Initial Temperature [K]
Tx = 293.15;        % Temperature Left and Right [K]
Tz = 293.15;        % Temperature Bottom [K]

% Initialize temperature field
T = T0 * ones(Nz, Nx);

% Transformation Variables
x_pulse = Lx / 2;
t_pulse = Nt*dt*0.55;

% Simulation loop
for n = 0:Nt
    % Calculate heat source term (pulse at the center)
    A = alpha * I0 * exp(-((((1:Nx) * dx) - x_pulse) / R0) .^2)...
        * exp(-(((n * dt) - t_pulse) / tau)^2);
    for i = 1:Nz-1
        depth_decay = exp(-alpha*(i-1)*dz);
        for k = 2:Nx-1
            if i==1
                T(i, k) = T(i, k)...
```

```

        + (((dt * Kappa) / (rho * Cp)) * ((T(i+1, k) - 2 * T(i,
k) + T0) / (dz ^ 2) + (T(i, k+1) - 2 * T(i, k) + T(i, k-1)) / (dx ^ 2)))...
        + (dt / (rho * Cp)) * A(1, k) * depth_decay;
    else
        T(i, k) = T(i, k)...
        + (((dt * Kappa) / (rho * Cp)) * ((T(i+1, k) - 2 * T(i,
k) + T(i-1, k)) / (dz ^ 2) + (T(i, k+1) - 2 * T(i, k) + T(i, k-1)) / (dx ^
2)))...
        + (dt / (rho * Cp)) * A(1, k) * depth_decay;
    end
end
end

% Boundary conditions (fixed temperature at boundaries)
T(end, :) = Tz;
T(:, 1) = Tx;
T(:, end) = Tx;

% Adjust temperature for melting
melting_mask = T > Tm;
melting_mask = logical(melting_mask - melting_mask1);
T = T - melting_mask * (Lf / Cp);
melting_mask1 = logical(melting_mask1 + melting_mask);

% Plot temperature distribution every time step
figure;
imagesc((1:Nx)*dx/1e-6, (1:Nx)*dz/1e-6, T)
title(['Temperature Distribution at t = ' num2str(n*dt/1e-9) 'ns']);
xlabel('X (micro meter)');
ylabel('Z (micro meter)');
colormap(gca, "default");
colorbar;
clim([290 82000]);
cb = colorbar();
ylabel(cb, 'Temperature (K)', 'Rotation', 270)
drawnow;
end

% Crater
evaporatedMask = T > Tb;
colorbar;
figure;
imagesc((1:Nx)*2, (1:Nx)*0.4, evaporatedMask)
xlabel('X (micro meter)');
ylabel('Z (micro meter)');
colormap(gca, "gray");
colorbar;
clim([0 1]);
cb = colorbar();
ylabel(cb, 'Ablated material', 'Rotation', 270)
drawnow;

```